

${}^4\text{He} + {}^4\text{He}$ elastic scattering at 158.2 MeVA. Nadasen, P. G. Roos, B. G. Glagola, G. J. Mathews,* V. E. Viola, Jr., H. G. Pugh,[†] and P. Frisbee*University of Maryland Cyclotron Laboratory, College Park, Maryland 20742*

(Received 31 August 1978)

Differential cross sections for the elastic scattering of ${}^4\text{He}$ from ${}^4\text{He}$ at 158.2 MeV are presented. These data along with data from lower energies are analyzed within the framework of an optical-model potential.

[NUCLEAR REACTIONS ${}^4\text{He}(\alpha, \alpha)$, $E_\alpha = 158.2$ MeV; measured $\sigma(\theta)$, $\theta = 10^\circ - 94^\circ$ c.m.; optical model analysis.]

For many years there has been considerable interest in reactions involving few-nucleon systems, since such relatively simple systems provide the opportunity for carrying out more fundamental calculations of the reaction. For example, a number of calculations have been performed using the resonating-group formalism with a realistic nucleon-nucleon interaction which describes low-energy nucleon-nucleon scattering. The success of such studies in providing a more complete understanding of nuclear reactions depends heavily on the availability of a large body of accurate experimental data on few-nucleon systems, particularly elastic scattering. In order to provide additional data on the ${}^4\text{He} + {}^4\text{He}$ system we have measured the elastic-scattering cross section at a laboratory energy of 158.2 MeV. These results extend the previous extensive measurements,^{1,2} which went up to 140 MeV.

A beam of 158.2 ± 0.5 MeV α particles from the University of Maryland Cyclotron with intensity varying from 1 to 200 nA was focused in the center of a 1.6 m diameter scattering chamber. The target consisted of a 12 cm diameter gas cell filled with high-purity helium gas to a pressure of approximately 1 atmosphere. The detection system consisted of a double-collimator system and a solid-state detector telescope. The collimator system, combined with the angular divergence of the beam and the multiple scattering in the target gas and gas-cell windows, provided an angular resolution of better than 0.8° [full width at half maximum (FWHM)] for all angles. The detector telescope consisted of a 1-mm Si surface-barrier ΔE detector and a 4-mm Si(Li) E detector rotated to 60° to produce an effective thickness of 8 mm. The signals from the two detectors were processed by conventional electronics, and the energy signals processed by an on-line IBM 360/44 computer. Both one- and two-dimensional analyzers were written on magnetic tape for subsequent analysis. Counting losses were measured via a $\Delta E - E$ pulser system

triggered by the beam current integrator.

Measurements of the ${}^4\text{He} + {}^4\text{He}$ differential cross sections were made over the laboratory angular range of 5° to 47° , corresponding to approximately 10° to 94° in the center-of-mass system. The laboratory angles were determined to an accuracy of better than $\pm 0.03^\circ$. Absolute cross sections were measured to better than 10%. The reliability of these measurements was checked by changing the beam energy to 118.6 MeV and comparing the measured ${}^4\text{He} + {}^4\text{He}$ elastic scattering cross sections to the previous work of Darriulat *et al.*¹ Agreement to within 5% was obtained.

The resultant measurements are presented in Fig. 1, along with data^{1,2} at three other energies. These data show systematic trends with energy such as the increasing slope and movement of the minima to smaller angles with increasing energy. In addition, the data at 158.2 MeV show a less pronounced minimum near 77° when compared to the 140 MeV data.

These data have been analyzed using the optical-model code of Chant³ which properly antisymmetrizes the two identical bosons. Two approaches to the optical-model analysis are possible. If one ignores possible forbidden bound states (due to the Pauli exclusion principle), the phase shifts $\delta_l(E)$ are zero at zero energy [$\delta_l(0) = 0$], and the $l=0$ and $l=2$ phase shifts become negative at higher bombarding energy. This behavior indicates a repulsive core in the $\alpha - \alpha$ interaction. Darriulat *et al.*¹ analyzed the phase shifts extracted from their data over an energy range from about 50 to 120 MeV using an energy-independent, but strongly l -dependent, potential with a repulsive-core radius of 1–2 fm. In terms of resonating-group calculations, the repulsive core arises from a nonlocal term whose source is the Pauli principle.

An alternative procedure has been suggested by Neudatchin *et al.*⁴ In particular they use a deep attractive potential which contains the $1s$, $2s$, and $1d$ forbidden bound states. In this case Swan⁵

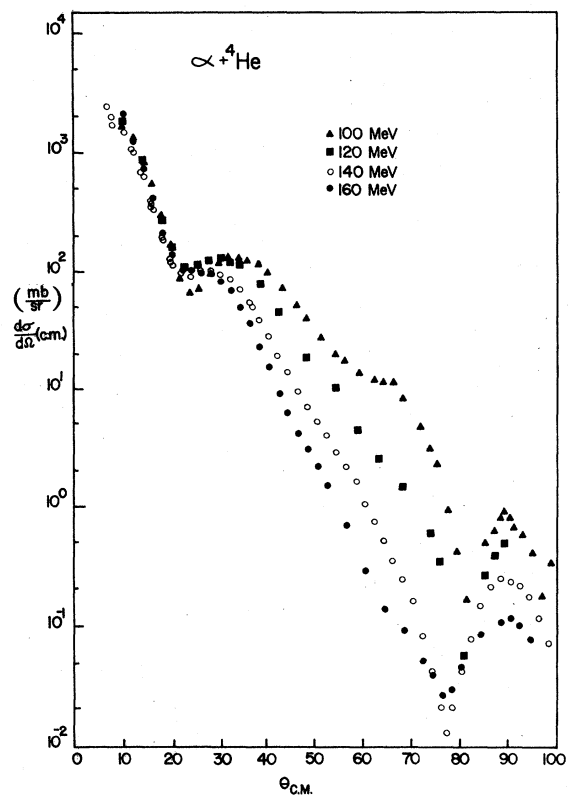


FIG. 1. $\alpha+{}^4\text{He}$ elastic scattering data at $E_{\text{lab}}=100, 120, 140,$ and 160 MeV.

has shown that the forbidden bound states should be included in Levinson's theorem. Thus at zero energy the phase shifts start as $\delta_0(0)=2\pi$, $\delta_2(0)=\pi$, and $\delta_{i>2}(0)=0$, and stay positive, removing the necessity for a repulsive core. Neudatchin *et al.*⁴ showed that they could reproduce rather well the α - α real phase shifts with such a deep real potential, particularly when an energy-dependent strength was included. It should be noted that no imaginary potential was included in their analysis. We have chosen to follow this procedure and analyze the present data, as well as data at lower energies, with a deep l -independent attractive potential. This was also the procedure followed by Frisbee² in the analysis of his 140-MeV data. The initial analysis was made with a com-

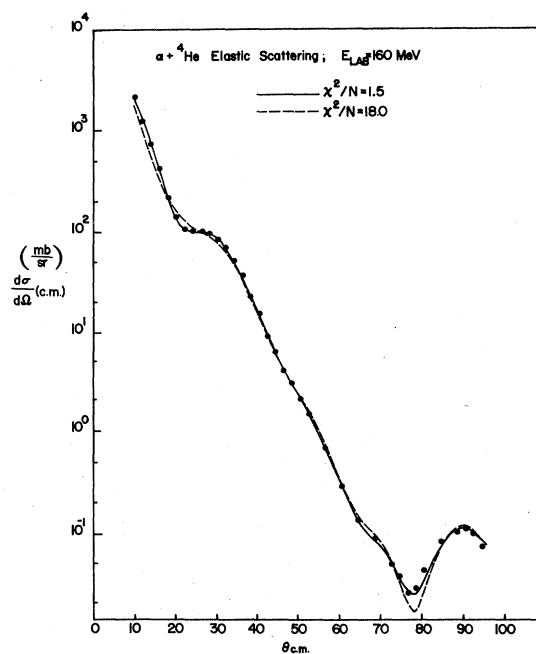


FIG. 2. Six- and nine-parameter optical model fits to the 160 MeV $\alpha+{}^4\text{He}$ data.

plex six-parameter Woods-Saxon well (Potential 1) of the form $Vf_1(r) + iW_v f_2(r)$ with $f_i = \{1 + \exp[(r - r_i 4^{1/3})/a_i]\}^{-1}$. The fit to the data is shown in Fig. 2 and the resultant parameters in Table I. N is the number of degrees of freedom (i.e., number of data points minus number of parameters). The fit is unsatisfactory, and the resultant parameters are similar to those obtained by Frisbee with a six-parameter Woods-Saxon potential. In particular for the real potential the radius parameter is small and the diffuseness large, leading to an almost exponential potential.

In order to improve the fit a second attractive real potential of Woods-Saxon form (parameters with primes) was added to provide more flexibility in the shape of the real potential (Potential 2). This procedure is similar to that used by Le Rigoleur and Perey⁶ who fitted the lower energy data using a real potential consisting of a sum of two attractive potentials, one Gaussian

TABLE I. Optical-model parameters for the fits to the data shown in Fig. 2 and described in the text.

	V	r_0	a_0	W_v	r_w	a_w	V'	r'_0	a'_0	χ^2/N
Pot 1	273.2	0.151	1.059	12.86	2.169	0.362				18.0
Pot 2	53.75	1.628	0.613	9.623	2.094	0.467	43.97	0.545	0.142	1.5

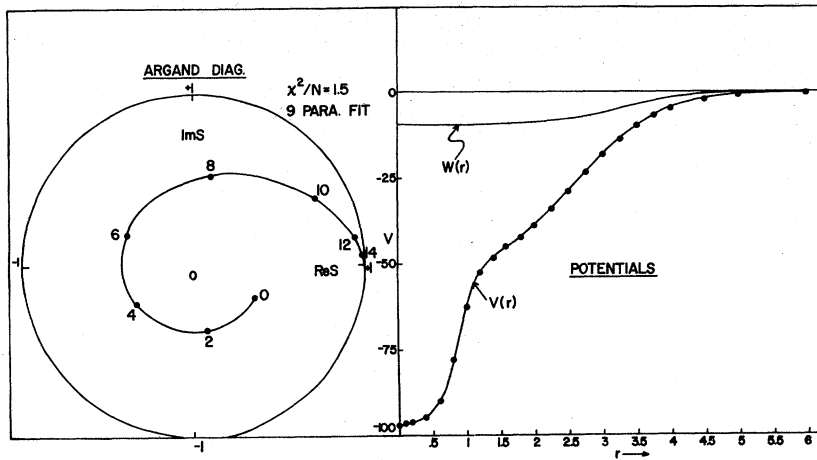


FIG. 3. Argand diagram and potentials for the nine-parameter optical-model fit.

and one Woods-Saxon. The results of this search are shown in Fig. 2 and Table I. Although we have introduced three new parameters, a significant improvement in the fit to the data is noted, producing a value of $\chi^2/N=1.5$. The resultant potential is shown in Fig. 3 and is again similar to that obtained by Frisbee with the same type of analysis. Although the kink in the potential is unphysical, we see that the flexibility provided by the sum of two real potentials allows the potential to break into two regions. At small radii the addition of a small radius ($r_0 = 0.545$ fm) and diffuseness ($a = 0.142$ fm) potential leads to a flat portion of the potential about 100 MeV deep for the first 0.5 fm. This region is most important for the low partial waves. The second potential is then free to describe the large-radius region

which dominates the higher partial waves.

The Argand diagram and radial distributions of the real and imaginary parts for Potential 2 are shown in Fig. 3. Compared to Potential 1 the lower partial waves ($l=0-8$) are less strongly absorbed, whereas the higher partial waves are more strongly absorbed. In addition the whole pattern is rotated significantly in the clockwise direction, reflecting the rather large change in the real potential.

The volume integrals of the potentials (Potential 2) obtained from our analysis of the 158.2 MeV data were found to be different from those of similar analysis by Frisbee,² indicating a possible energy dependence. To investigate this energy dependence further, we have analyzed the data at 53.4, 77.55, 99.6, 119.86, 140, and 158.2 MeV in a consistent manner using the two-component real potential. Because the geometrical parameters at the different energies showed very little scatter and because of our conviction that the geometry of the interaction should be energy independent, we further fixed the geometrical parameters to be $r_0, a_0, r'_0, a'_0, r_w, a_w = 1.66, 0.61, 0.59, 0.17, 2.1, 0.4$ fm, respectively. The real and imaginary volume integrals obtained are shown as a function of center-of-mass energy in Fig. 4. Definite trends with energy are indicated by both. Although there is some scatter in the real potential volume integral $J_R/4A$, a linear energy dependence with an energy coefficient of -1.3 ± 0.3 MeV fm³/MeV is consistent with the results of the analysis. This energy dependence compares well with the value of -1.0 ± 0.3 determined from the results of Singh *et al.*,⁷ for $\alpha + {}^{24}\text{Mg}$ and -1.5 ± 0.3 quoted by Smith *et al.*,⁸ for $\alpha + {}^{12}\text{C}$. Excluding the 140 MeV data we obtain a more accurately defined linear energy dependence of $+1.2 \pm 0.2$ MeV fm³/MeV for the imaginary

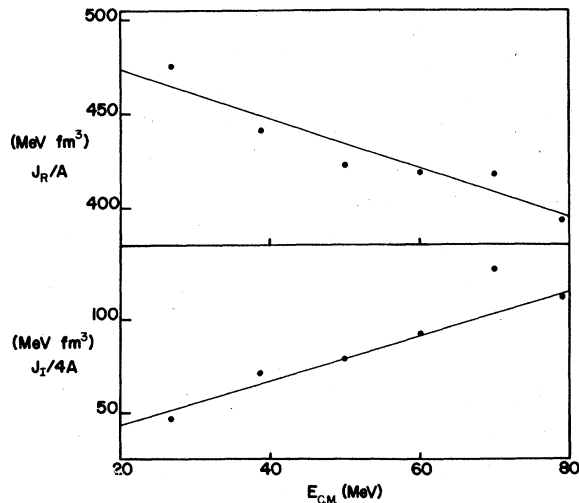


FIG. 4. Energy dependence of the real and imaginary volume integral per nucleon pair.

volume integral $J_1/4A$, in excellent agreement with the value of 1.3 ± 0.4 obtained by Singh *et al.*⁷

These data provide additional information on the ${}^4\text{He} + {}^4\text{He}$ system at high energies which can be used to test current theories of few-nucleon systems. A phenomenological analysis of the data shows that good fits to the data can be obtained, as long as one allows more flexibility in

the shape of the real potential.

The authors gratefully acknowledge the University of Maryland Computer Science Center for their generous allocation of computer time. This work was supported in part by the National Science Foundation and Department of Energy.

*Present address: Lawrence Berkeley Laboratory, Berkeley, California.

†Present address: National Science Foundation, Washington, D. C.

¹P. Darriulat, G. Igo, H. G. Pugh, and H. D. Holmgren, Phys. Rev. **137**, B315 (1965).

²P. Frisbee, Ph.D. thesis, University of Maryland, 1972 (unpublished).

³N. S. Chant, private communication.

⁴V. G. Neudatchin, V. I. Kukulin, V. L. Korutkikh, and V. P. Korennoy, Phys. Lett. **34B**, 581 (1971).

⁵P. Swan, Proc. R. Soc. **228**, 10 (1955); Ann. Phys. (N.Y.) **48**, 455 (1968).

⁶Le Rigoleur and F. G. Perey, private communication.

⁷P. P. Singh, P. Schwandt, and G. C. Yang, Phys. Lett. **59B**, 113 (1975); G. C. Yang, Ph.D. thesis, Indiana University, 1975 (unpublished).

⁸S. M. Smith, *et al.*, Nucl. Phys. **A207**, 273 (1973).